Supporting Information

Cobalt-based silica nanospheres for enhanced peracetic acid activation: The efficiency and mechanism to degrade tetracycline hydrochloride

Hongyan Wu et al.

Summary

Table S3. The characteristic parameters of tap water, lake water and river water.

Text S1. HPLC conditions for pollutant concentrations.

An Agilent TC-C18 C18 column (4.6 × 250 mm) was utilized. The detection wavelength was set at 355 nm, the column temperature was maintained at 35°C, and the mobile phase flow rate was fixed at 1 mL/min. TCH was detected using a mobile phase of 0.1% formic acid/acetonitrile at a ratio of 80%/20% (v/v), with an injection volume of 10 μL. In contrast, for CTC, OTC, and MO, the mobile phase ratio of 0.1% formic acid/acetonitrile was adjusted to 60%/40% (v/v).

Text S2. Toxicity evaluation experimental procedure.

Select 50 black bean seeds of comparable weight. First, soak them in 75% ethanol for 30 s to cleanse. Then promptly immerse them in distilled water, gently agitating for 30 s. Repeat this process three times to remove residual alcohol. After rinsing with Solution 1, place the seeds in a hollowed-out culture container. Next, measure 100 mL of Solution A and pour it evenly into the container. Finally, place the container in natural conditions (approximately 25°C) for dark cultivation. Observe growth trends at 24 h, 48 h, and 96 h, adding 100 mL of Solution A each time. Replace Solution 1 with Solutions 2, 3, and 4, respectively, and repeat the above process. Each treatment group includes three replicates. Compare the growth of black beans cultivated in the four solutions.

Text S3. Test and characterization methods.

Scanning electron microscope (SEM, Hitachi Regulus 8230, Japan), X-ray diffraction (XRD, D8 ADVANCE, Germany) and Raman spectroscopy (Raman, WITec alpha300R, Germany) were used to measure the prepared materials to analyze their physicochemical properties. Elemental distribution was analyzed using an energy-dispersive X-ray spectrometer (EDS). Detailed structural analysis was performed using a FEI Tecnai G2 F20 S-Twin high-resolution transmission electron microscope (HRTEM) operating at 200 kV to investigate crystalline phases and lattice structures. Radical trapping experiments were performed by electron paramagnetic resonance (EPR, Bruker A300, Germany) spectrometry. Surface chemical states were analyzed by X-ray photoelectron spectroscopy (XPS) on a Thermo Fisher Scientific K-Alpha system with monochromatic Al Kα radiation under 1.5×10^{-9} Torr vacuum. The intermediates of TCH transformation were detected by liquid chromatography-mass spectrometry (LC-MS, Thermo Fisher Scientific Ultimate 3000 UHPLC -Q Exactive, USA). The concentrations of PAA and H_2O_2 in PAA stock solution were measured using titration method as previously described,[1] and the residual PAA and H_2O_2 in the PAA working solution was monitored by a modified spectrophotometric method according to our previous research.[2] An examination of total organic carbon (TOC) was conducted using the Shimadu TOC-L CPH from Japan to measure the degree of mineralization. The leaching of cobalt (Co) and the cobalt content in the catalyst were examined using a Agilent 7850 (MS) (U.S.) inductively coupled plasma optical emission spectrometer (ICP-OES).

Text S4. Calculation equations for the contributions of different reactive species to TCH reactivity of Co@SiO_2/PAA system.

The contribution of each ROS to the oxidation of TCH in the Co@SiO_2/PAA system was quantitatively assessed using a radical probe method. The corresponding calculation equations are as follows:

$$kt = \ln\left(\frac{C_{TCH,0}}{C_{TCH,t}}\right) \#(1)$$

$$CR_{\cdot OH/R-O\cdot} \approx \frac{k_{blank} - k_{MeOH}}{k_{blank}} \#(2)$$

$$CR_{R-O\cdot} \approx \frac{k_{blank} - k_{2,4-HD}}{k_{blank}} \#(3)$$

$$CR_{CH_3C(O)OO\cdot} \approx \frac{k_{blank} - k_{Mn^{2+}}}{k_{blank}} \#(4)$$

$$CR_{^1O_2} \approx \frac{k_{blank} - k_{FFA}}{k_{blank}} \#(5)$$

$$CR_{\cdot OH} \approx \frac{k_{blank} - k_{TBA}}{k_{blank}} \#(6)$$

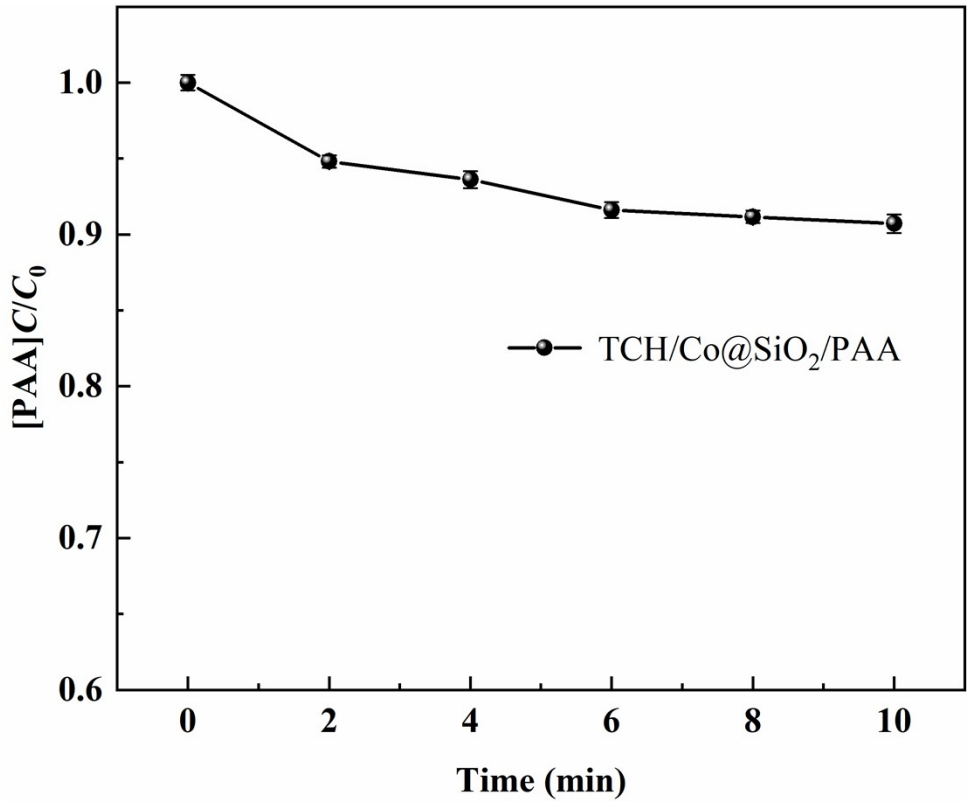

Fig. S1. Consumption curves of PAA in TCH/Co@SiO_2/PAA systems. Conditions:TCH = 10 mg/L, PAA = 0.5 mM, Co@SiO_2 = 200 mg/L, initial pH = 7, temperature = 25 °C.

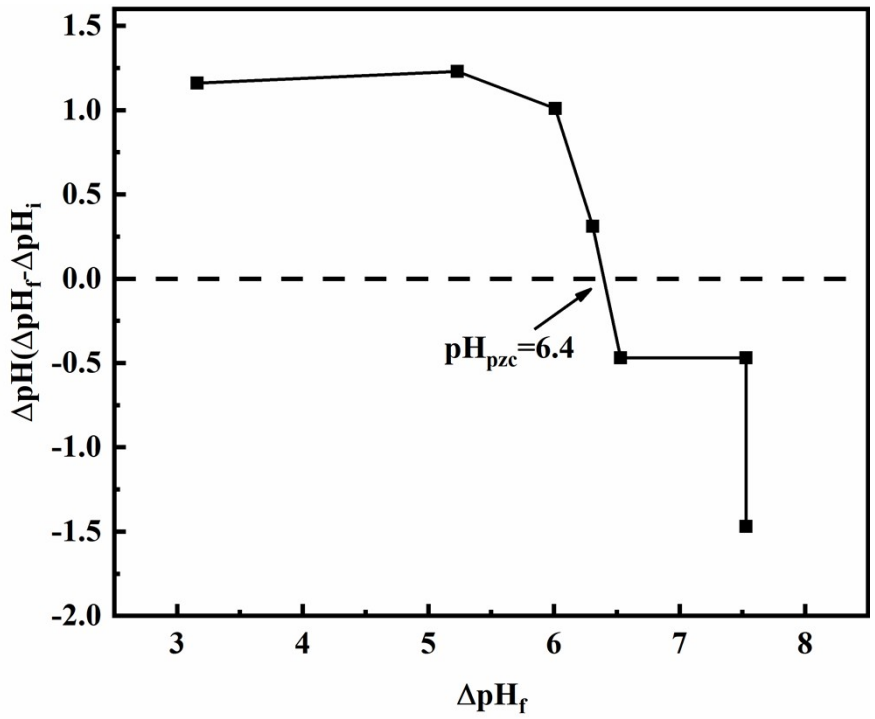

Fig. S2. Zeta potential of $Co@SiO_2$.

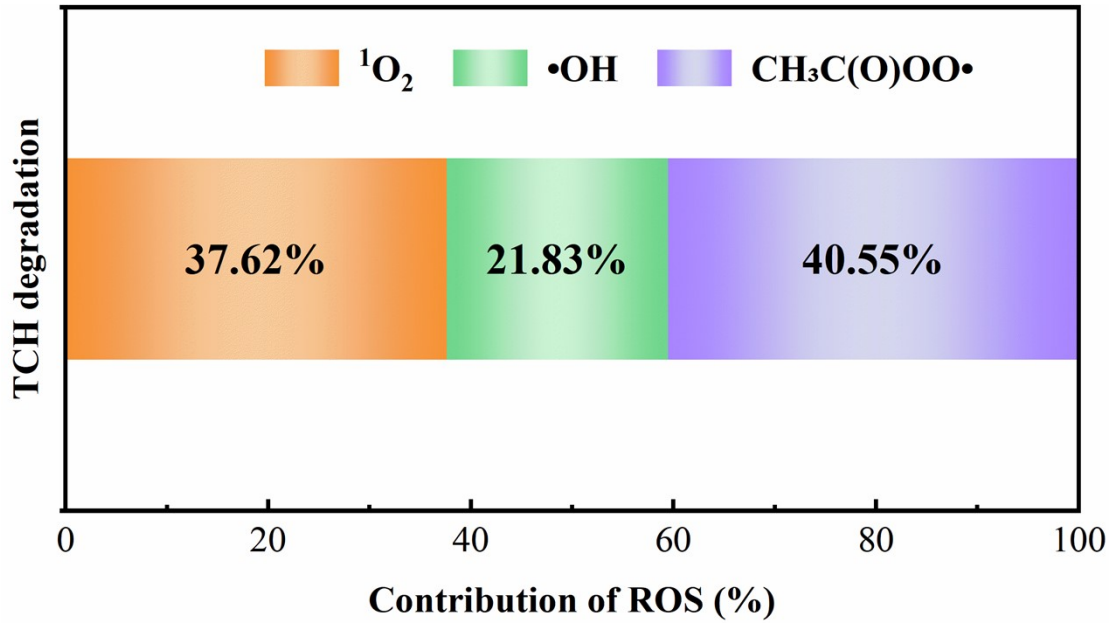

Fig.S3. Contributions of ROS on TCH degradation in the Co@SiO_2/PAA system.

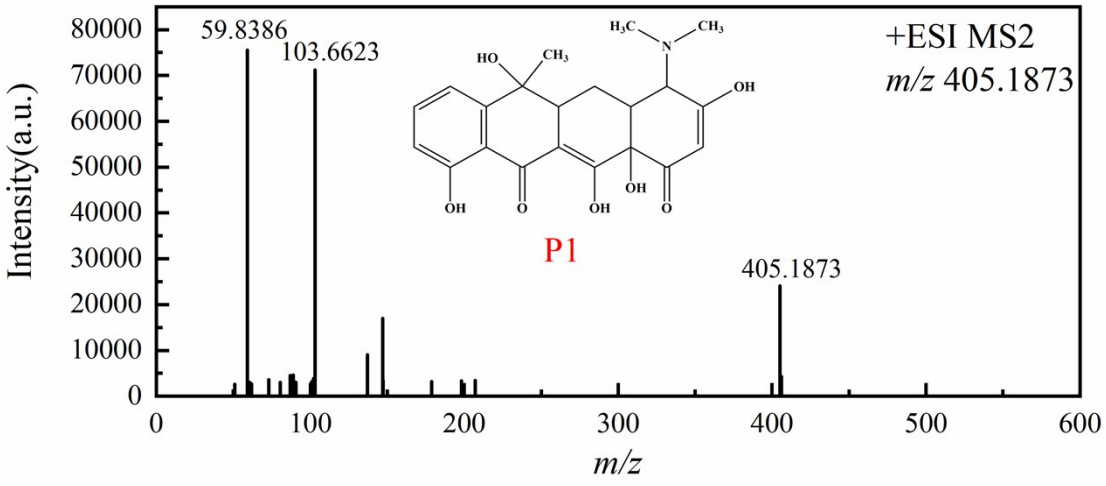
Intensity(a.u.)
80000
70000
60000
50000
40000
30000
20000
10000
0
59.8386
103.6623
405.1873
+ESI MS2
m/z 405.1873
P1
0
100
200
300
400
500
600
m/z

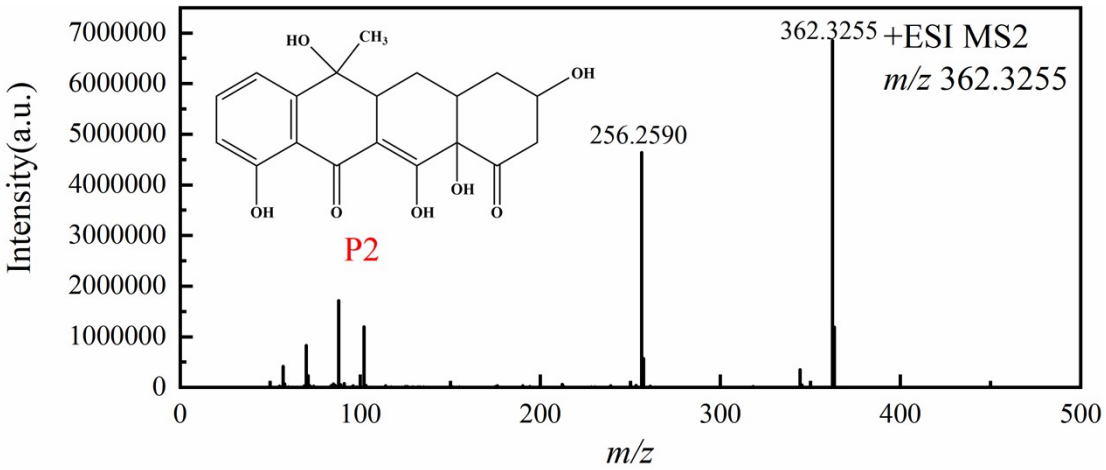
Intensity(a.u.)
7000000
6000000
5000000
4000000
3000000
2000000
1000000
0
362.3255
256.2590
+ESI MS2
m/z 362.3255
P2
0
100
200
300
400
500
m/z

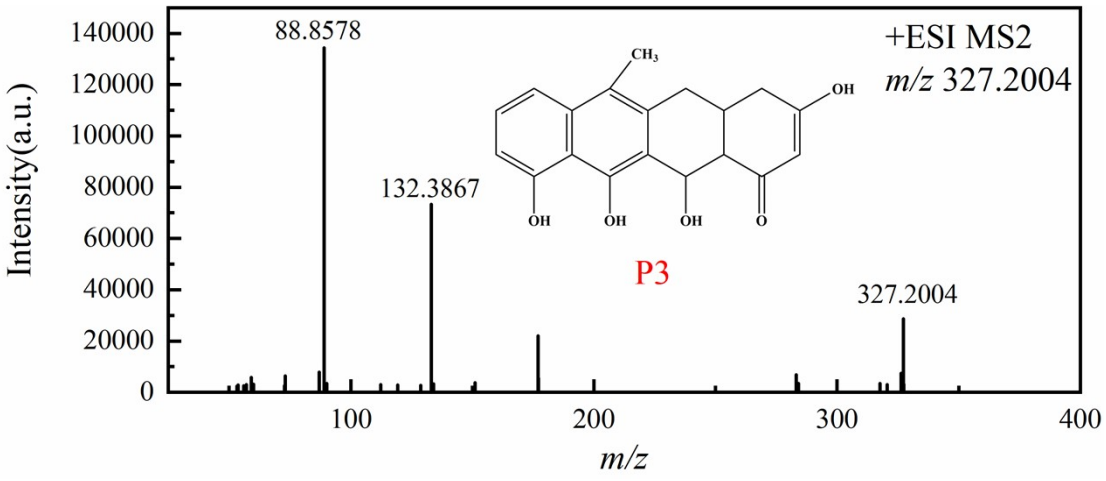
Intensity(a.u.)
140000
120000
100000
80000
60000
40000
20000
0
88.8578
132.3867
327.2004
+ESI MS2
m/z 327.2004
P3
100
200
300
400
m/z

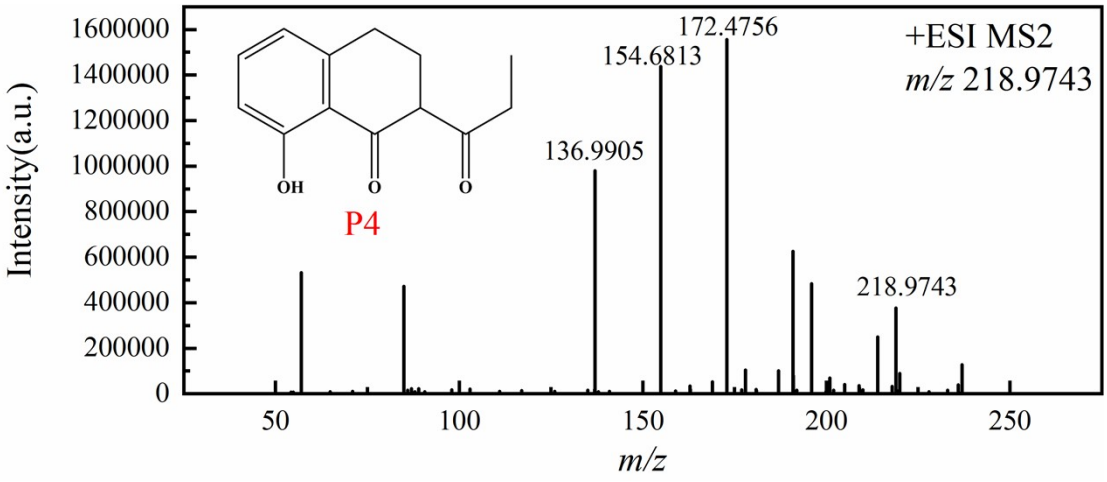
+ESI MS2
m/z 218.9743
172.4756
154.6813
136.9905
218.9743
P4
Intensity(a.u.)
m/z

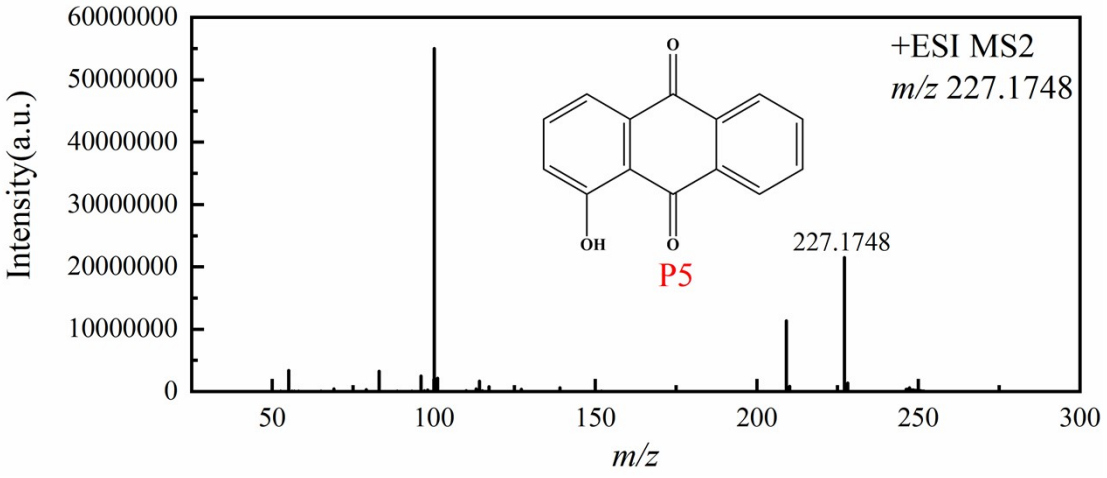
+ESI MS2
m/z 227.1748
227.1748
P5
Intensity(a.u.)
m/z

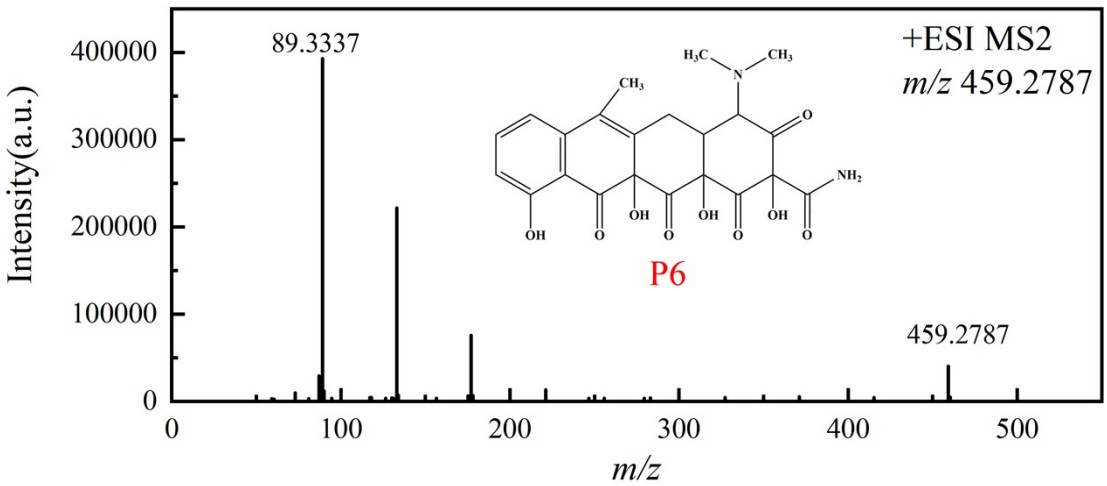
+ESI MS2
m/z 459.2787
89.3337
459.2787
P6
Intensity(a.u.)
m/z

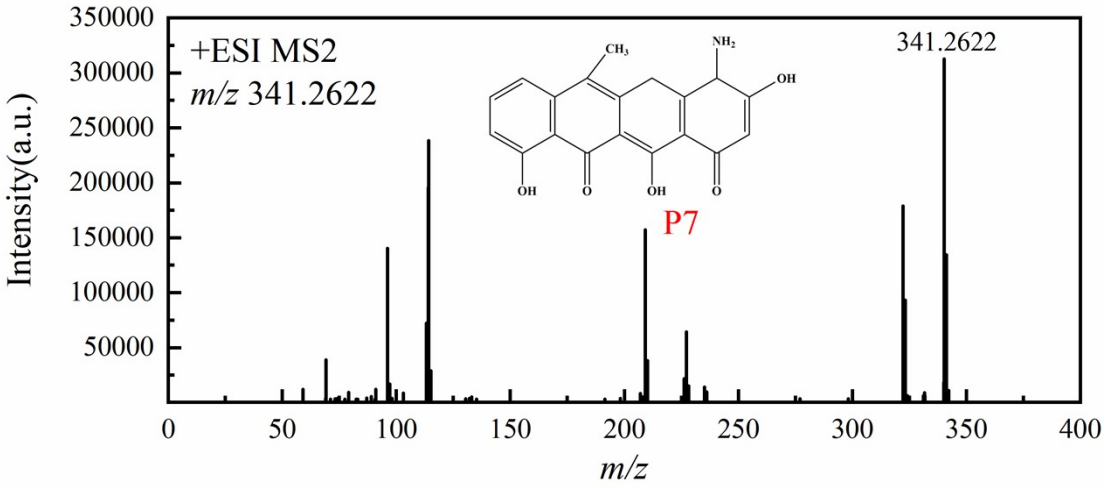
+ESI MS2
m/z 341.2622
341.2622
P7
Intensity(a.u.)
m/z

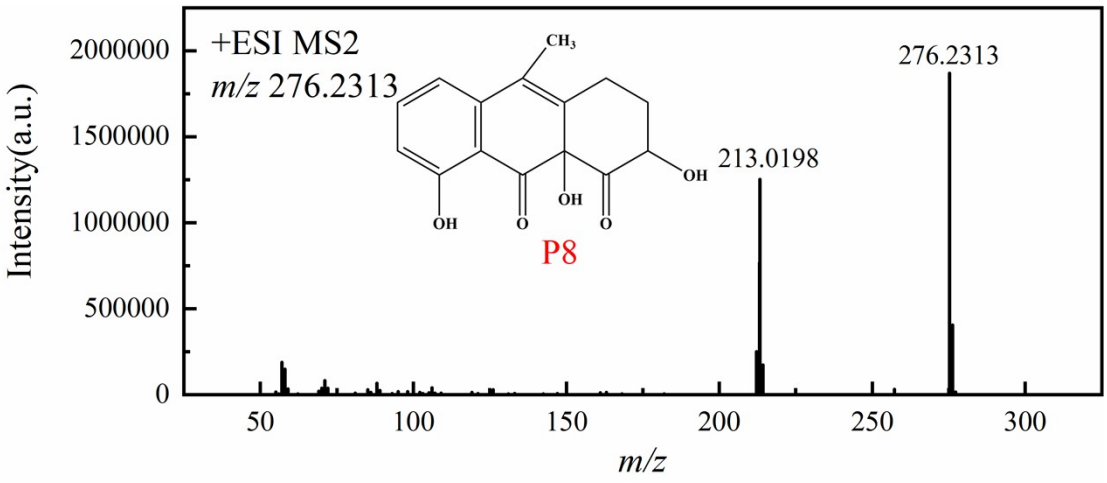
+ESI MS2
m/z 276.2313
276.2313
213.0198
P8
Intensity(a.u.)
m/z

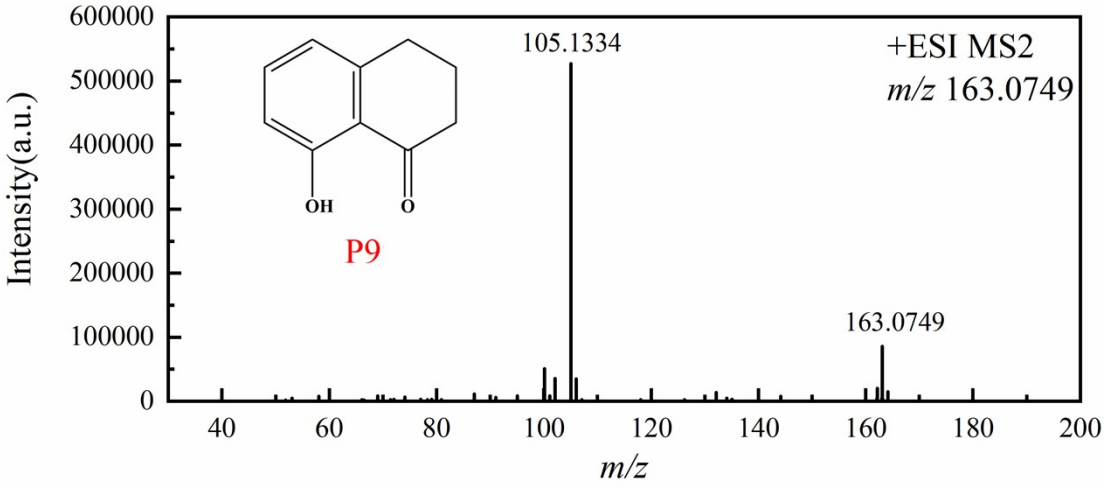
+ESI MS2
m/z 163.0749
105.1334
163.0749
P9
Intensity(a.u.)
m/z

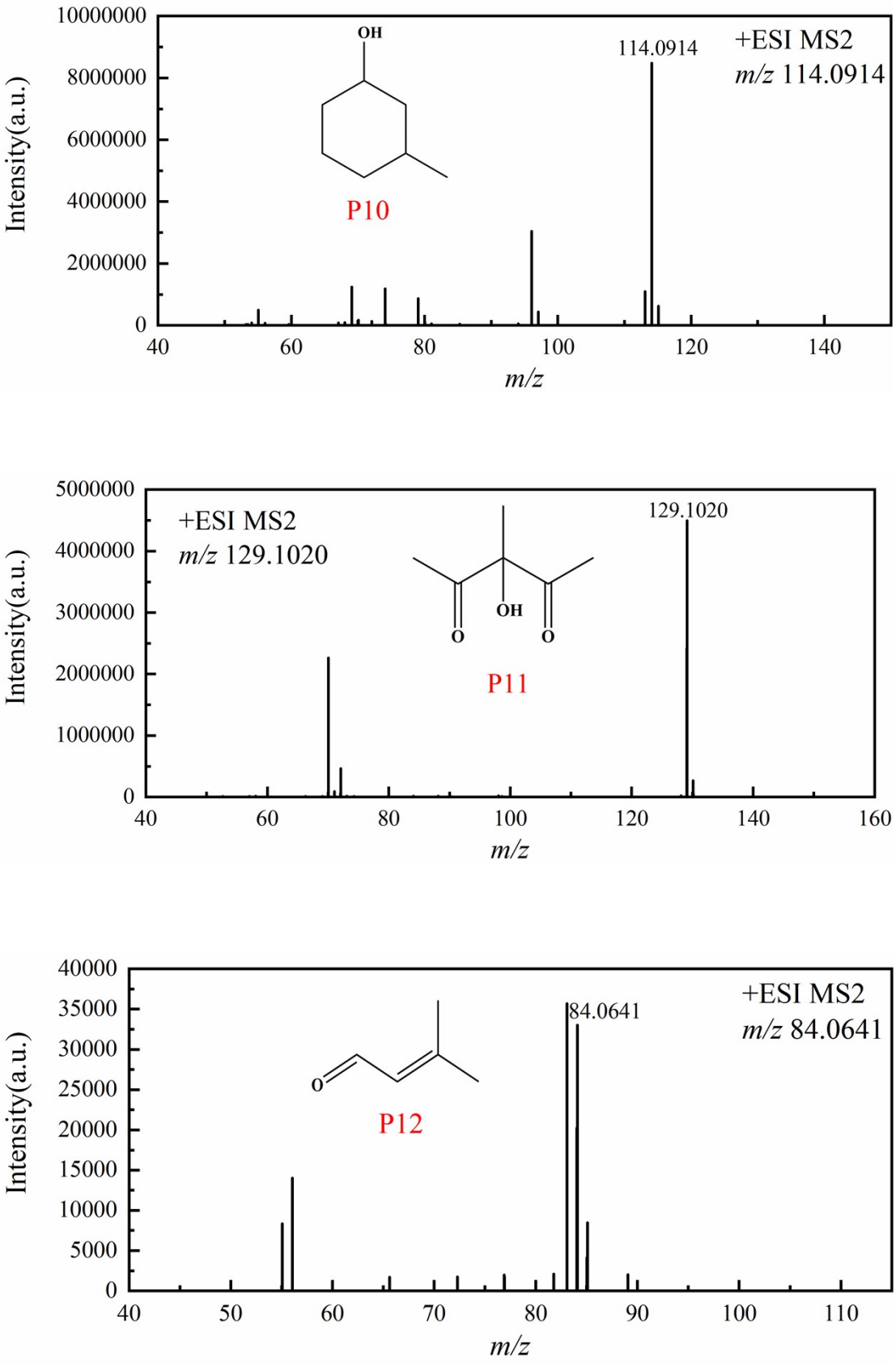

Fig. S4. The MS and MS^2 spectra of TCH and intermediates.

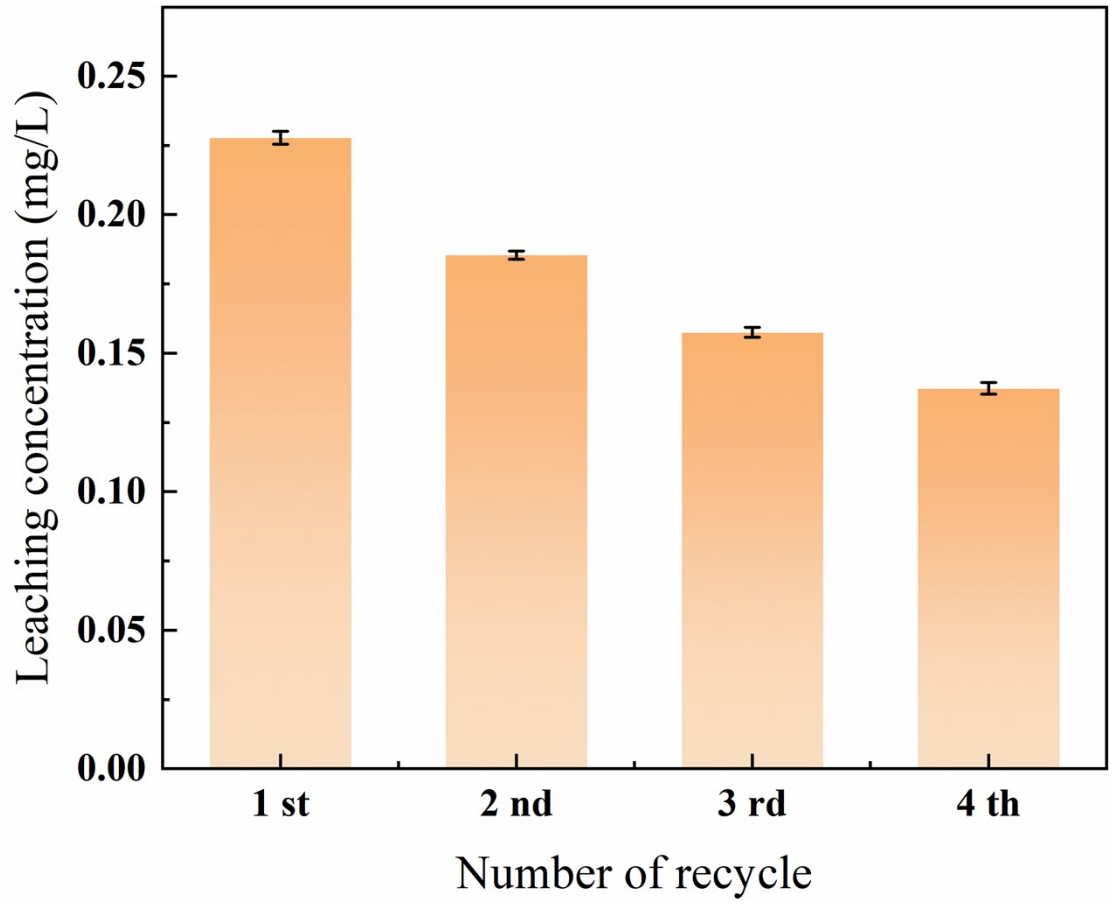

Fig. S5. Leaching concentrations of cobalt ions after each cycle. Reaction conditions: TCH = 10 mg/L, PAA = 0.5 mM, Co@SiO_2 = 200 mg/L, initial pH = 7, temperature = 25 °C.

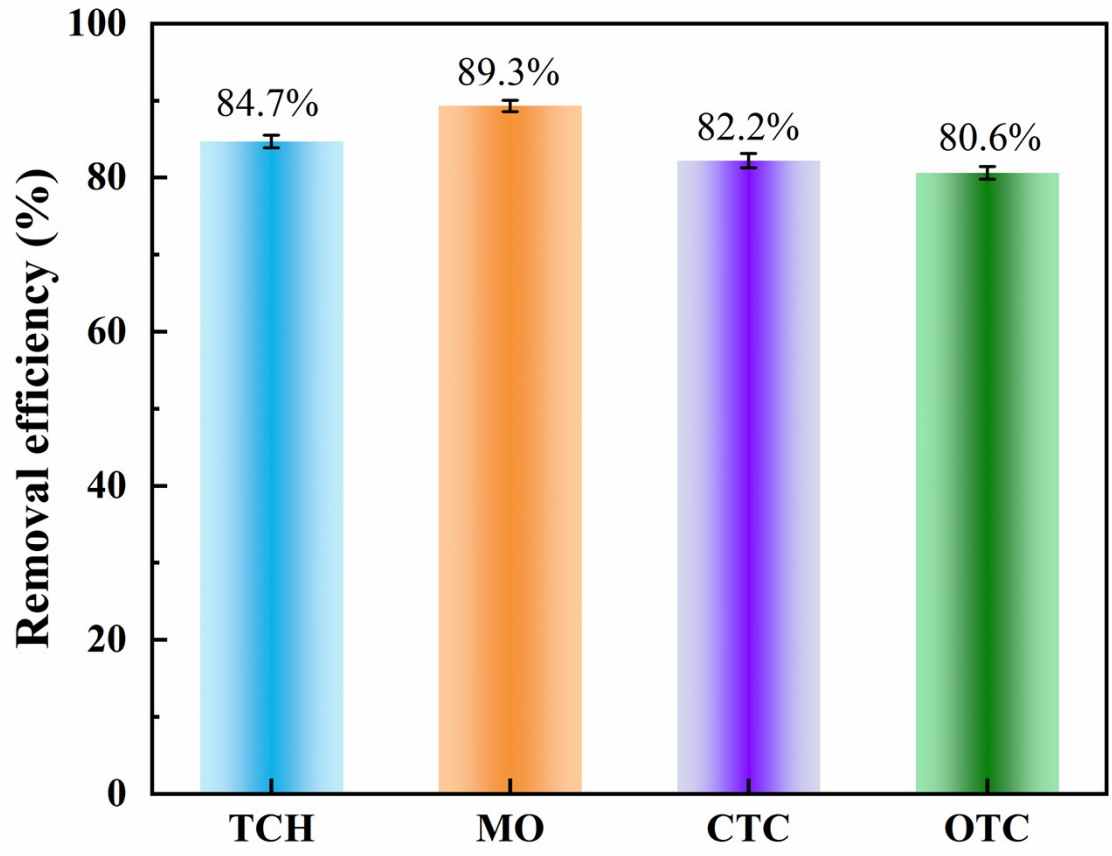

Fig. S6. The removal efficiency of other organic pollutants by the Co@SiO_2/PAA system. Reaction conditions: Co@SiO_2 = 200 mg/L, PAA= 0.5 mM, TCH= CTC = OTC = MO = 10 mg/L, temperature = 25 ℃, pH = 7.

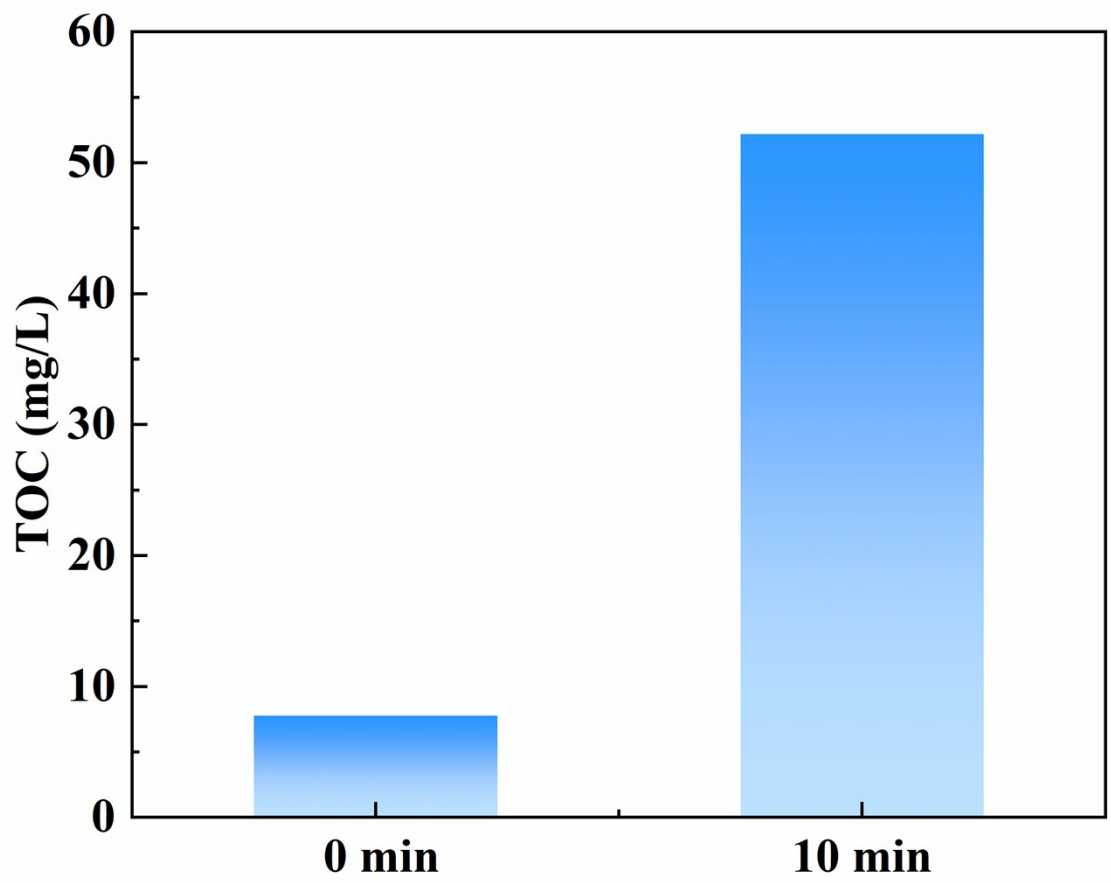

Fig. S7. Changes of TOC in the degradation of TCH by Co@SiO_2/PAA system. Reaction conditions: TCH = 10 mg/L, PAA = 0.5 mM, Co@SiO_2 = 200 mg/L, initial pH = 7, temperature = 25 °C.

Table S1. Comparison of cobalt-based catalysts for the degradation of organic pollutants.

Pollutant	**C_0**	**Catalyst**	**PAA Dose (mM)**	**Time (min)**	**K_{obs} (min^{-1})**	**Removal efficiency**	**Ref.**
SMX	10 μM	$CoFe_2O_4$	0.2	30	0.0465	87.3%	3
TCH	10 mg/L	$FeCo_2S_4$/AC	1	20	0.099	94.12%	4
RhB	50 mg/L	$CoFe_2O_4$@N−C	0.5	30	0.166	98%	5
SDZ	10 mg/L	Co-K-N-O-C	0.1	50	0.046	100%	6
SMR	20μM	CoFe-LDH	0.2	30	0.067	82.3%	7
SDZ	20 μM/L	Co_3O_4-in-CNTs	0.23	5	1.33	100%	8
SMX	100 mg/L	BFC5O	0.1	30	0.102	96.2%	9
TCH	50 μM	Co_{NC}-CNF	0.15	60	-	55.5%	10
TCH	10 mg/L	Co@SiO_2	0.5	10	0.1751	84.7%	This work

Table S2. The structural information of the intermediate products.

Product number	*m/z*	Molecule formula	Possible structure
P1	405	$C_{21}H_{23}O_7N$	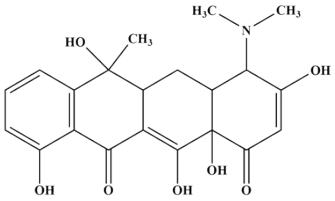
P2	362	$C_{19}H_{20}O_7$	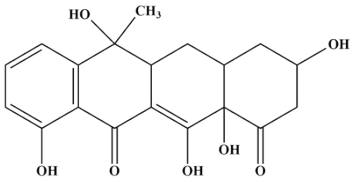
P3	327	$C_{19}H_{18}O_5$	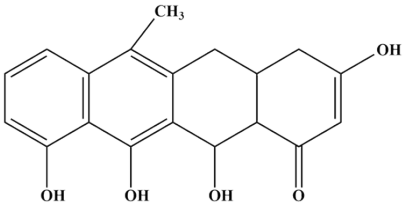
P4	218	$C_{13}H_{14}O_3$	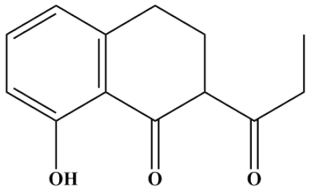
P5	227	$C_{14}H_8O_3$	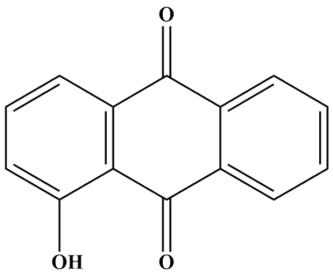
P6	459	$C_{22}H_{22}O_9N_2$	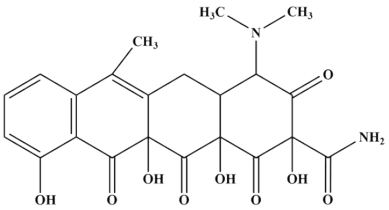
P7	341	$C_{19}H_{15}O_5$	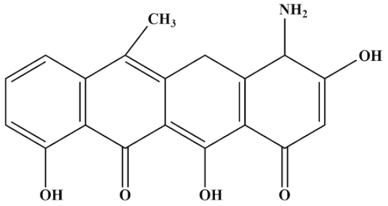

P8	276	$C_{15}H_{14}O_5$	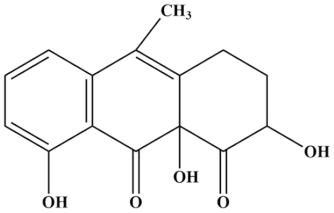
P9	163	$C_{10}H_{10}O_2$	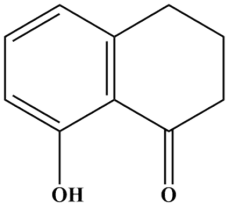
P10	114	$C_7H_{14}O$	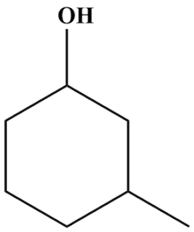
P11	129	$C_6H_{10}O_3$	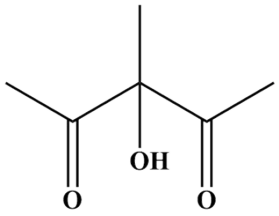
P12	84	C_5H_8O	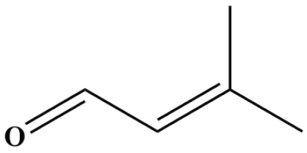

Table S3. The characteristic parameters of tap water, lake water and river water.

Parameter	Unit	Tap water	Lake water	River water
pH	1	6.83	7.21	7.28
NH_3-N	mg/L	0.08	0.1	0.08
TN	mg/L	1.16	1.67	2.1
COD	mg/L	2.8	10.4	16.5

References

1 S. Chen, M. Cai, Y. Liu, L. Zhang and L. Feng, Effects of water matrices on the degradation of naproxen by reactive radicals in the UV/peracetic acid process, *Water Res.*, 2019, **150**, 153-161.

2 Z. Wang, J. Wang, B. Xiong, F. Bai, S. Wang, Y. Wan, L. Zhang, P. Xie and M. R. Wiesner, Application of cobalt/peracetic acid to degrade sulfamethoxazole at neutral condition: efficiency and mechanisms, *EnST*, 2019, **54**, 464-475.

3 J. Wang, B. Xiong, L. Miao, S. Wang, P. Xie, Z. Wang and J. Ma, Applying a novel advanced oxidation process of activated peracetic acid by $CoFe_2O_4$ to efficiently degrade sulfamethoxazole, *Appl. Catal., B*, 2021, **280**, 119422.

4 Y. Zhang, Z. Cheng, Q. Zhang, R. Wang, X. Sun, W. Xue and Q. Zeng, Non-radical activation of peracetic acid by Fe-Co sulfide modified activated carbon for the degradation of refractory organic matter, *J. Environ. Chem. Eng.*, 2024, **12**, 114258.

5 Z. Zhang, W. Chen, X. Wang, R. Yan, Y. Xie and S. Wei, Degradation of Rhodamine B by magnetic nitrogen-doped carbon covered cobalt ferrite ($CoFe_2O_4$@N−C) activated peracetic acid: Emphasizing partially covered, performance and mechanism, *J. Water Process Eng.*, 2025, **77**, 108352.

6 N. Bux, H. Guo, S. H. Tumrani, R. A. Soomro, Q. Ma, J. Zhou and T. Wang, Variable-valence Co-activated peroxyacetic acid induced rapid sulfadiazine degradation and mineralization: Co^{2+}/Co^{3+} redox cycling, *Chem. Eng. J.*, 2025, 168329.

7 Z.-H. Xie, C.-S. He, Y.-L. He, S.-R. Yang, S.-Y. Yu, Z. Xiong, Y. Du, Y. Liu, Z.-C. Pan, G. Yao and B. Lai, Peracetic acid activation via the synergic effect of Co and Fe in CoFe-LDH for efficient degradation of pharmaceuticals in hospital wastewater, *Water Res.*, 2023, **232**, 119666.

8 Y. Liu, Y. Wang, X. Li, X. Zhang, M. Fang, L. Zheng, Y. Li, J. Ren, H. Guo, Q. Ma, J. Zhou and T. Wang, Multi-path accelerating sulfadiazine degradation via peracetic acid oxidation induced by nanoconfined co species: Highlighting electron rearrangement effect, *Chem. Eng. J.*, 2024, **494**, 153167.

9 S. Liu, Z. Lian, Q. Yu, G. Wang, F. Di, F. Ma and D. Han, Cobalt-doped $Bi_2Fe_4O_9$ nanosheets effectively enhance peracetic acid activation for sulfamethoxazole degradation: Performance and mechanism, *Chem. Eng. J.*, 2025, **522**, 166844.

10 S. Xia, J. Chang, Y. Cai, Z. Shi, L. Deng and H. Zhang, Cobalt nanocluster-anchored carbon nanofibers for peracetic acid activation: Dual-radical/nonradical pathways toward efficient roxarsone degradation, *Chem. Eng. J.*, 2025, **525**, 170063.